Clinical Neurophysiology 165 (2024) 127–137

Contents lists available at ScienceDirect

Clinical Neurophysiology

journal homepage: www.elsevier.com/locate/clinph

Volumetric and functional connectivity changes of the thalamic nuclei in different stages of Alzheimer's disease

Emre Hari [a,b,c,*,1], Cigdem Ulasoglu-Yildiz [d,c,1], Elif Kurt [d,c], Ali Bayram [d,c], Hakan Gurvit [e], Tamer Demiralp [b,c]

[a] Graduate School of Health Sciences, Istanbul University, 34216 Istanbul, Turkey
[b] Department of Physiology, Istanbul Faculty of Medicine, Istanbul University, 34093 Istanbul, Turkey
[c] Hulusi Behcet Life Sciences Research Laboratory, Neuroimaging Unit, Istanbul University, 34093 Istanbul, Turkey
[d] Department of Neuroscience, Aziz Sancar Institute of Experimental Medicine, Istanbul University, 34093 Istanbul, Turkey
[e] Department of Neurology, Behavioral Neurology and Movement Disorders Unit, Istanbul Faculty of Medicine, Istanbul University, 34093 Istanbul, Turkey

HIGHLIGHTS

- We examined volumetric and functional connectivity changes in the thalamus in Alzheimer's disease.
- Medial group nuclei are significantly affected in Alzheimer's disease.
- The thalamo-frontal and thalamo-occipital connections are affected in Alzheimer's disease.

ARTICLE INFO

Article history:
Accepted 23 June 2024
Available online 9 July 2024

Keywords:
Alzheimer's disease
Thalamic Nuclei
Volumetric analysis
Functional magnetic resonance imaging
Functional connectivity

ABSTRACT

Objective: Memory processes known to be impaired in Alzheimer's disease (AD) are maintained by a large-scale neurocognitive network with subcortical components, including the thalamus. Therefore, we aimed to examine the volumetric and functional changes of the thalamic nuclei at different scales across AD stages.
Methods: MRI data of patients diagnosed with 20 AD dementia (ADD), 30 amnestic mild cognitive impairment (MCI), and 30 subjective cognitive impairment (SCI) were used. Volumetric and functional connectivity analyzes were performed by dividing the thalamus into anterior, medial, posterior, lateral and intralaminar nucleus groups and their specific subnuclei.
Results: In the course of AD, the volume of the medial group nuclei, especially the mediodorsal medial magnocellular (MDm) nucleus, decreases. Medial group nuclei and MDm functional connectivity with frontal areas were decreased both in ADD and MCI compared to SCI group, while both of them increased their functional connectivity with visual areas in the ADD group compared to the MCI group.
Conclusions: Our study suggests that the medial group of the thalamus, and specifically the MDm, may be affected in AD.
Significance: Specific thalamic nuclei may be a critical anatomical region for investigating structural and functional changes in AD.
© 2024 International Federation of Clinical Neurophysiology. Published by Elsevier B.V. All rights are reserved, including those for text and data mining, AI training, and similar technologies.

1. Introduction

Alzheimer's disease (AD) is a neurodegenerative process with progressive cognitive impairment. Although preceded by a decades-long amyloid deposition during the pre-clinical stage, neuronal loss, thus, clinical symptoms are closely related to the appearance of neurofibrillary tangles (NFTs) (Jack et al., 2010). In the typical AD phenotype that accounts for 90% of the cases, the transentorhinal cortex and hippocampo–entorhinal complex is

* Corresponding author at: Primary Postal address: Department of Physiology, Istanbul Faculty of Medicine, Istanbul University, 34093 Fatih-İstanbul, Turkey.
E-mail addresses: emrehr@hotmail.com (E. Hari), cigdemulasoglu@gmail.com (C. Ulasoglu-Yildiz), elifkurt@istanbul.edu.tr (E. Kurt), ali.bayram@istanbul.edu.tr (A. Bayram), gurvit@istanbul.edu.tr (H. Gurvit), demiralp@istanbul.edu.tr (T. Demiralp).
[1] These authors contributed equally to this work and share first authorship.

https://doi.org/10.1016/j.clinph.2024.06.018
1388-2457/© 2024 International Federation of Clinical Neurophysiology. Published by Elsevier B.V. All rights are reserved, including those for text and data mining, AI training, and similar technologies.

the initial target of NFTs, giving rise to the progressive spread along the nodes of the episodic memory neural network, which includes intrinsic hippocampal circuitry and the larger Papez circuit (Braak et al., 2011; Braak and Braak, 1991). This spread pattern is reflected clinically by early progressive amnesia, which, in the later stages, is associated with multiple cognitive deficits, and dementia as the NFTs spread to the neocortex. The initial stage can be further subdivided into subjective cognitive impairment (SCI) and mild cognitive impairment (MCI) stages according to the detection of objective memory loss in the latter.

Starting with the paradigm shift during the last decade of the previous century, the network approach to the brain-behavior relationship replaced the older centrist/localizationist approach. Accordingly, different cognitive domains are no longer localized within the dedicated cortical centers but within the large-scale distributed neural networks, which contain not only cerebral cortical nodes but also subcortical components, such as cerebellar, thalamic, and striatal (Mesulam, 1990). This shift radically changed the conception of subcortical structures. Thalamus is no longer a mere sensory-relay station of an ascending sensory pathway on its voyage from the peripheral sensory receptor to its primary cortex; likewise, the striatum is no longer a mere motor-relay station on the descending motor pathway. The cortical parcellation of sensory-motor and cognitive functions is also true for the cerebellum, striatum, and thalamus (Buckner et al., 2011; Choi et al., 2012; Hwang et al., 2017; Yeo et al., 2011). So, different subnuclei of the thalamus are components of different neural networks.

The thalamic component of the Papez circuit is the anterior thalamic nuclei (ATN). It receives afferents via the mamillo-thalamic tract and sends efferents to the posterior cingulate and retrosplenial cortices via the ventral thalamo-cingulate bundle. The amnestic state resulting from anterior thalamic infarctions due to polar artery occlusion is well-established (Cipolotti et al., 2008; Schmahmann, 2003). The mediodorsal nucleus (MD) is put forward as "another candidate owing to its dense connections with subhippocampal structures" (Danet et al., 2015). Especially, magnocellular MD in addition to being the main communicant of the orbitofrontal cortex is reciprocally connected with those "subhippocampal paralimbic structures," namely, the entorhinal, perirhinal, and the parahippocampal cortices (Mitchell and Chakraborty, 2013; Mitchell, 2015; Pergola et al., 2018).

In addition to the typical presenting findings of hippocampal volume reduction in Alzheimer's disease, it has also been reported that the thalamus suffers from volume loss in the disease (Bernstein et al., 2021; Shi et al., 2009; Zidan et al., 2019). Moreover, postmortem studies revealed that certain pathological changes were also observed in specific thalamic nuclei in the early stages of the disease (Bobinski et al., 1999; Roh et al., 2011). Even before hippocampal atrophy, atrophy of the thalamus and the caudate nucleus has been reported in patients with presymptomatic familial AD (Ryan et al., 2013). Recently, the corticothalamic network was suggested as having "the potential to be a master regulator of diverse cognitive and behavioral domains that are affected in AD" (Jagirdar and Chin, 2019). Hypoconnectivity within the default mode network (DMN), which consists of the medial prefrontal cortex, the posterior cingulate cortex as the major cortical hubs and the inferior parietal lobules, lateral temporal cortex, and the hippocampal formation as the other cortical nodes is an early sign of the disease (Spreng et al., 2010; Zhou and Seeley, 2014). ATN and MD were previously suggested as the components of the DMN (Alves et al., 2019).

In this context, we hypothesize that specific thalamic nuclei will be affected both structurally and functionally at different stages of Alzheimer's disease. On the other hand, other thalamic nuclei interconnected with modality-specific sensorimotor cortices would be relatively intact. Furthermore, considering that functional connectivity changes precede atrophic changes between different stages of the disease, altered functional connectivity (both hypoconnectivities and compensatory hyperconnectivities) of these thalamic subnuclei may be more pronounced (Alves et al., 2019). Therefore, this study aimed to investigate the sensitivity of thalamic subnuclei to progressive neurodegeneration during Alzheimer's disease by using advanced segmentation methods on anatomical and functional MRI data.

2. Materials and methods

2.1. Participants

The study included 20 participants diagnosed with ADD, 30 with MCI, and 30 with SCI who were followed up in the Department of Neurology, Behavioral Neurology and Movement Disorders Unit of Istanbul University, Istanbul Faculty of Medicine. All participants were assessed using the Mini-Mental State Examination (MMSE), Clinical Dementia Rating (CDR), Free and Cued Selective Reminding Test (FCSRT) (Buschke, 1984; Folstein et al., 1975; Ivnik et al., 1997; Morris, 1991) and geriatric depression scale (Ertan et al., 1997; Yesavage et al., 1982). Clinical diagnosis was made in three patient groups using neuropsychological test scores. Additionally, T2-weighted and FLAIR MRI images of all participants were examined by an experienced neurologist for hyperintensity and high resolution T1-weighted coronal images were used to determine the medial temporal lobe atrophy (MTA) scores (Scheltens et al., 1992).

For the ADD group, patients were diagnosed according to the typical ADD clinical criteria of the National Institute on Aging and Alzheimer's Association (NIA-AA), and participants with a CDR score of 0.5 or 1 and without any neuropsychiatric diagnosis other than dementia were included (McKhann et al., 2011). In the diagnosis of MCI, the memory score threshold value, which has a high probability of turning into ADD, was preferred (Grober et al., 2010). Therefore, the MCI group consisted of patients diagnosed with MCI, according to the Petersen criteria, with a CDR score of 0.5 and an FCSRT-total free recall (TFR) score of 24 or less (Grober et al., 2010; Petersen, 2004). Participants with subjective memory complaints with a CDR score of 0 and an FCSRT-TFR score higher than 24 were included in the SCI group (Jessen et al., 2014). On the other hand, participants with current or past neurological or psychiatric disorders that could negatively affect cognition, comorbid major depression, major head trauma accompanied by loss of cognition, white matter T2/FLAIR hyperintensity with Fazekas scores greater than 1 on clinical MRI examinations, as well as contraindications for MRI scanning were excluded from the study.

2.2. MRI acquisition

The structural MRI images were acquired at Hulusi Behcet Life Sciences Research Laboratory, Istanbul University, using a 3-Tesla magnetic resonance imaging system (Phillips, Achieva, Best, The Netherlands) equipped with a 32-channel SENSE head coil. High-resolution T1-weighted structural images were recorded with 3D TFE (Turbo Field Echo) sequence in the axial plane (aligned with the anterior commissure-posterior commissure line) with the following parameters: Total scan time: 5 min 55 s, time of repetition/-time of echo: 8.3/3.8 ms, flip angle: 8°, field of view: 220 × 240 mm, matrix: 252 × 227, 180 axial slices (with no gap), reconstructed to 1 mm^3 isotropic voxels. Resting-state functional MRI data were recorded with echo-planar imaging (EPI) sequence in the axial plane (anterior commissure-posterior commissure aligned) with the following parameters: TR / TE: 3000 / 30 ms, FOV: 212 × 199 mm, flip angle: 80°, acquisition matrix size:

64 × 59, voxel size: 3.31 × 3.31 × 3. 31 mm, 195 volumes, each containing 48 axial slices covering the whole brain, were obtained with a total scan time of 10 min.

2.3. Structural MRI analysis

Structural MRI data were segmented using FreeSurfer (https://surfer.nmr.mgh.harvard.edu, version Dev 6.0.0). Firstly, FreeSurfer standard *recon-all* steps were applied to the individual structural data of all participants (Fischl et al., 2002). After this stage, each participant's skull-stripping and segmentation processes were visually inspected using Freeview. In the next step, detailed segmentation was performed to obtain 25 thalamic nuclei using the thalamus atlas created by Iglesias and colleagues (2018) based on high-resolution MRI and histological data (Iglesias et al., 2018). Subsequently, volume values per thalamic nuclei derived from this atlas were calculated for each participant. The obtained 25 thalamic nuclei were grouped anatomically, and 6 major groups were formed (Iglesias et al., 2018). Thalamic nuclei are grouped as follows:

i. **Anterior group:** anteroventral (AV) nucleus,
ii. **Lateral group:** laterodorsal (LD), lateral posterior (LP) nuclei
iii. **Ventral group:** ventral anterior (VA), ventral anterior magnocellular (VAmc), ventral lateral anterior (VLa), ventral lateral posterior (VLp), ventral posterolateral (VPL), ventromedial (VM) nuclei
iv. **Intralaminar group:** central medial (CeM), central lateral (CL), paracentral (Pc), centromedian (CM), parafasicular (Pf) nuclei
v. **Medial group:** paratenial (Pt), medial ventral-reuniens (MV-re), mediodorsal medial magnocellular (MDm), mediodorsal lateral parvocellular (MDl) nuclei
vi. **Posterior group:** lateral geniculate (LGN), medial geniculate (MGN), limitans-suprageniculate (L-SG), pulvinar anterior (PuA), pulvinar medial (PuM), pulvinar lateral (PuL), pulvinar inferior (PuI) nuclei

Thalamic subgroups are shown in three dimensions in Fig. 1. The ratio of each segment volume-to-estimated total intracranial volume (eTIV) was calculated and used in further statistical analysis to adjust for potential inter-individual head size differences.

2.4. Functional MRI analysis

Preprocessing steps were performed using CONN functional connectivity toolbox version 18b (https://web.conn-toolbox.org/) (Nieto-Castanon, 2020; Whitfield-Gabrieli and Nieto-Castanon, 2012) and SPM 12 (Statistical Parametric Mapping version 12; https://www.fil.ion. ucl.ac.uk/spm12/) (Penny et al., 2011). Initially, the functional images were realigned to the first image to correct for within-scan head movement. The Artifact Detection Tools (ART) toolbox was then used to check for potential outlier scans representing excessive head motion or signal intensity spikes (Behzadi et al., 2007). For this purpose, 5 standard deviations from the mean intensity of the entire session as used for the global-signal z-value threshold. 0.9 mm threshold or greater differences from the previous scan as used for the composite motion difference criteria. Having been coregistered with the functional images, the structural images were segmented into white matter, gray matter, and cerebrospinal fluid (Friston et al., 1995). The individual transformation matrix was obtained during the normalization step of the structural data to the Montreal Neurological Institute (MNI) standard space and used for the spatial normalization of the functional images (Friston et al., 1995). Finally, the functional data resampled to 2 × 2 × 2 mm voxels were smoothed by spatial convolution with an isotropic Gaussian kernel (full-width half maximum = 8 mm).

The denoising procedure of the CONN toolbox, including a linear regression of potential noise effects in the BOLD signal and temporal band-pass filter (Nieto-Castanon, 2020), was applied to the functional data to remove the impact of potential noise sources such as movement and physiological effects. Using an anatomical component-based noise correction (aCompCor), method instead of the removal of global signal (Behzadi et al., 2007), potential noise components derived from WM and CSF signals were estimated and subsequently included as confounds in the denoising step in addition to six motion parameters obtained in the realignment step and their first order derivatives of twelve motion components. Furthermore, outlier scans of subjects defined with ART in the preprocessing step were included as potential noise effects. Finally, the impact of the scanning session was included in confounding effects to decrease the influence of slow, linear trends in the BOLD signal (Nieto-Castanon, 2020). Then a 0.01 - 0.1 Hz bandpass filter was applied to the functional images to filter effects from noise sources.

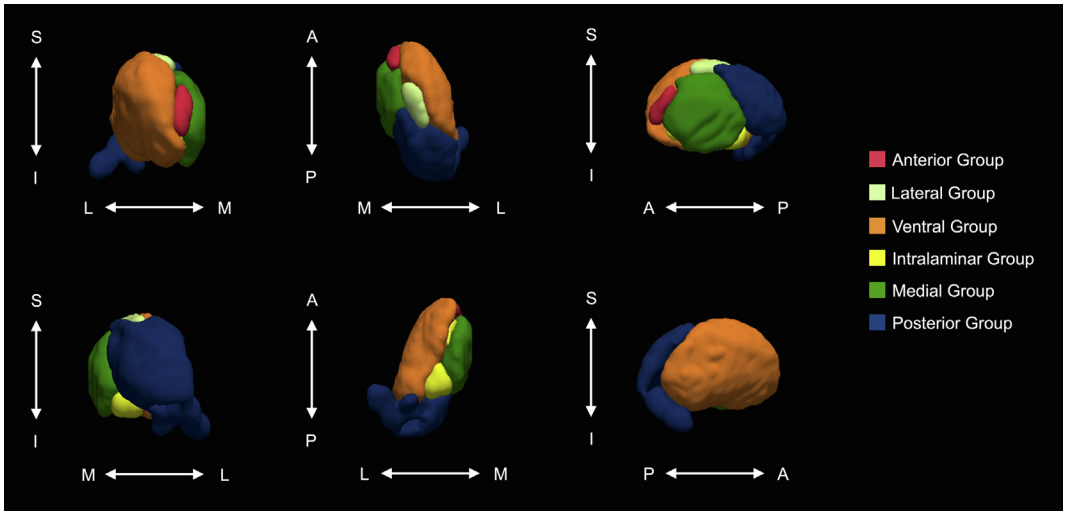


Fig. 1. 3D representation of thalamic nuclei; I: Inferior; S: Superior; A: Anterior; P: Posterior; M: Medial; L: Lateral.

Since the most prominent morphometric changes from the thalamic nuclei obtained as a result of the segmentation process were in the medial group nuclei and MDm, these thalamic nuclei were chosen as the region of interest (ROI) for seed-to-voxel functional connectivity analysis. Segmentation was performed using the MNI 2 mm standard space FreeSurfer pipeline to generate thalamic nuclei seeds. After the segmentation stage, medial group and MDm nuclei seeds were obtained (Fig. 2). Functional connectivity changes of ROIs were compared between the three groups using analysis of variance (ANOVA) at the second level, with $p_{unc} < 0.001$ at the voxel level and family-wise error (FWE) adjusted $p_{FWE} < 0.0125$ at the cluster level. The significance threshold was set as $p_{FWE} < 0.017$ in pairwise comparisons by applying Bonferroni correction.

2.5. Statistical analysis

Statistical analyses were conducted on the volumetric values of normalized thalamic nuclei using the SPSS (IBM SPSS Statistics version 26, https://www.ibm.com/tr-tr/products/spss-statistics) statistical program. Analysis of covariance (ANCOVA) was applied by controlling the effect of age, education, and gender with the group as an independent/between-subject factor.

In the first step, the total volumes of the thalamic subgroups for each hemisphere were compared; then, in the second step, differences in the thalamic subnuclei were examined. By applying Bonferroni correction for multiple comparisons, the significance threshold was set as $p < 0.0042$ (for 6 thalamic subgroups x 2 hemispheres, 0.05/12 = 0.0042) for thalamic subgroups and $p < 0.001$ (for 25 thalamic subnuclei x 2 hemispheres, 0.05/50 = 0.001) for thalamic subnuclei. Bonferroni correction was also applied for post hoc analysis of anatomical regions that showed significant differences in ANCOVA results. In addition, linear regression analysis was performed to predict the memory scores on FCRST-TFR using the significant volumetric changes observed in the AD progress as independent variables.

Demographic, clinical, and volumetric data were first examined using the Shapiro-Wilk test to determine whether they followed a normal distribution. One-way analysis of variance (ANOVA) with post hoc comparisons was performed using Bonferroni correction for the normally distributed data. For the data without normal distribution and/or containing outliers, the Kruskal-Wallis H test, and post-hoc pairwise comparisons were performed using the Mann-Whitney *U* test with Bonferroni correction for multiple comparisons. The Chi-square test was performed to examine the gender distribution between the groups.

3. Results

3.1. Demographic and clinical results

Demographic and clinical statistical analysis results of the groups included in the study are given in Table 1. No statistically significant differences were found among the 3 groups in terms of education, age, gender ratio or depression scores (Respectively, $\chi^2 = 1.647$, $p = 0.439$; $\chi^2 = 3.209$, $p = 0.201$; $\chi^2 = 4.469$, $p = 0.107$; $F(2,77) = 0.757$, $p = 0.473$).

There were statistically significant differences between the 3 groups in terms of FCSRT-TFR scores ($F(2,77) = 111.984$, $p < 0.001$), MMSE scores ($\chi^2 = 36.122$, $p < 0.001$) and MTA scores ($\chi^2 = 30.343$, $p < 0.001$). In post hoc comparisons, while the SCI group performed better than the MCI ($p < 0.001$) and ADD ($p < 0.001$) groups in terms of FCSRT-TFR scores, the MCI group also performed better than the ADD group ($p < 0.001$). Likewise, in post

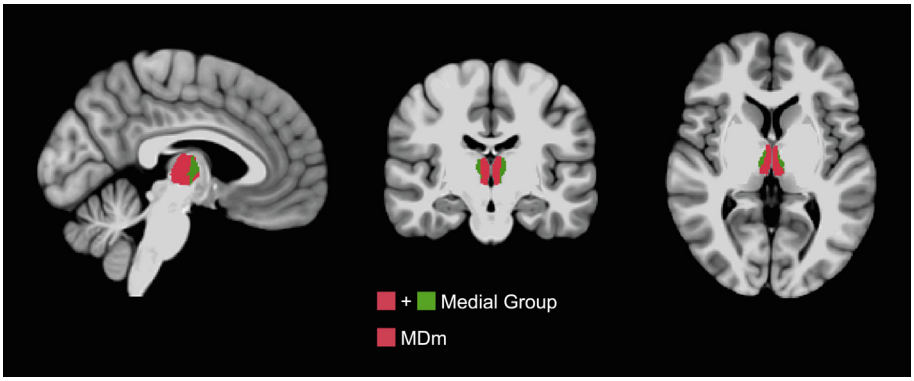


Fig. 2. Sagittal, coronal, and axial sections of an MNI 152 template showing the medial group and mediodorsal medial magnocellular nuclei seeds. The green and red colors represent the medial group, and only the red represents the mediodorsal medial magnocellular nucleus. MDm: Mediodorsal medial magnocellular. (For interpretation of the references to colour in this figure legend, the reader is referred to the web version of this article.)

Table 1
Demographic and clinical characteristics of the groups.

	Mean ± standard deviation				Post hoc results		
	SCI (n = 30)	MCI (n = 30)	ADD (n = 20)	Test	SCI vs. ADD	SCI vs. MCI	MCI vs. ADD
Age	62.57 ± 7.93	63.90 ± 7.63	67.40 ± 10.19	3.209[c]	-	-	-
Gender(F/M)	11 / 19	19 / 11	11 / 9	4.469[b]	-	-	-
Education	13.07 ± 4.83	11.20 ± 4.96	11.15 ± 4.54	1.647[c]	-	-	-
GDS	7.00 ± 4.80	6.52 ± 4.61	8.39 ± 6.11	0.757[a]	-	-	-
MTA[d]	0 [0 – 2]	1 [0 – 2]	2 [1 – 4]	30.343[c]	$p < 0.001$	$p = 0.063$	$p < 0.001$
MMSE	29.03 ± 1.24	27.90 ± 1.69	23.20 ± 3.85	36.122[c]	$p < 0.001$	$p = 0.044$	$p < 0.001$
FCSRT-TFR	30.53 ± 4.13	18.23 ± 4.46	8.40 ± 7.34	111.984[a]	$p < 0.001$	$p < 0.001$	$p < 0.001$

SCI: Subjective cognitive impairment; MCI: Mild cognitive impairment; ADD: Alzheimer's disease dementia; F: Female; M: Male; MMSE: Mini-Mental State Examination; FCSRT-TFR: Free and Cued Selective Reminding Test-Total Free Recall; GDS: Geriatric Depression Scale; MTA: Medial Temporal Lobe Atrophy; [a]One-way ANOVA, *p*-values were Bonferroni corrected for multiple comparisons; [b]Chi-square; [c]Kruskal-Wallis H test and Mann-Whitney *U* test for post hoc comparisons using Bonferroni correction; [d]Median [minimum–maximum] values were presented. The significance threshold was set as $p < 0.05$.

hoc comparisons of MMSE, the SCI group performed better than the MCI (U = 257.500, p = 0.044) and ADD (U = 33.500, p < 0.001) groups, and the MCI group also performed better than the ADD (U = 80.000, p < 0.001) group. There was also significant difference among the groups in terms of the MTA score. Post hoc comparisons revealed that the MTA score of the ADD group was higher than both those of the MCI (U = 114.500, p < 0.001) and SCI (U = 53.000, p < 0.001) groups, while no statistically significant difference was detected between the MCI and SCI groups (U = 310.000, p = 0.063).

3.2. Volumetric results of the thalamic subgroups and nuclei

ANCOVA revealed a significant difference between the groups only in the medial group of each left and right thalamus (Table 2, Fig. 3). Post-hoc pairwise comparisons showed that compared to the ADD group, the SCI group had larger volumes of both left and right medial nuclei, while the MCI group had only a larger left medial nuclei volume (SCI vs. ADD: p = 0.0014 for left; p = 0.0003 for right; MCI vs. ADD: p = 0.008). MCI vs ADD comparisons were not significantly different (Fig. 3).

Further comparison to scrutinize which nucleus within the medial group was mainly responsible for the volumetric differences between the groups revealed significant differences only for the left and right MDm (p = 0.0002; p = 0.0001, respectively) (Table 3). Post hoc comparisons showed that both the SCI group and the MCI group had larger volumes for both left and right MDm than ADD group (SCI vs. ADD: p = 0.0003; p = 0.00007, respectively; MCI vs. ADD: p = 0.004; p < 0.024, respectively), MCI vs ADD comparisons were not significantly different (Fig. 3). Statistical analysis results of all thalamic nuclei are given in Appendix Table A1.

3.3. Linear regression analyses

To investigate to what extent the medial nuclei and MDm nucleus predicted memory scores, linear regression analyses were performed using each left and right MDm and medial group nuclei volume as the dependent and FCRST-TFR scores as the independent variables. The left medial group nuclei volume (R = 0.463, R^2 = 0.215, F(1,78) = 21.321, p < 0.001) explained the memory performance by 20%, while the right medial group nuclei volume (R = 0.469, R^2 = 0.220, F(1,78) = 21.940, p < 0.001) explained 21%. On the other hand, the left MDm volume (R^2 = 0. 265, F(1, 78) = 28.187, p < 0.001) explained 26% while the right MDm volume (R^2 = 0. 246, F(1, 78) = 25.445, p < 0.001) explained 24% of the variance in the memory performance.

3.4. Functional connectivity analyses findings

The MDm nucleus and medial group nuclei of the left and right thalami that demonstrated significant volume differences between the groups in the structural analysis were defined as ROIs to be used as seed regions in the seed-to-voxel functional connectivity analysis. Separate ANCOVAs across the three groups revealed significant group effects for the bilateral medial group nuclei, and bilateral MDm nuclei.

The left medial group nuclei seed showed altered FC with the left superior frontal gyrus. In the post-hoc comparisons, ADD group demonstrated increased FC with the bilateral lingual gyri, right intracalcarine, lateral occipital, and cuneal cortices compared to the MCI groups. On the other hand, the left medial group FC to bilateral medial frontal, superior frontal, and paracingulate gyri, and the right frontal pole was decreased in the ADD group compared to the SCI group. No significant FC differences were found between the MCI and SCI groups (Table 4; Fig. 4). Similarly, the right medial group nuclei seed showed altered FC with the left superior frontal gyrus across the three groups. Post-hoc comparisons revealed decreased FC in the ADD group with the bilateral medial frontal gyri, left superior frontal gyrus, and right paracingulate gyrus compared to the SCI. No significant FC difference was found in the SCI vs. MCI and MCI vs. ADD comparisons (Table 4, Fig. 4).

When we used the left MDm as the seed region, ANCOVA showed altered FC with the right paracingulate cortex and bilateral superior and medial frontal gyri. Post-hoc comparisons revealed that the ADD group demonstrated increased FC with the bilateral lingual gyri, right intracalcarine cortex, right lateral occipital cortex, right cuneal cortex, and right occipital pole compared to the MCI group. On the other hand, in the ADD group, FC was decreased in bilateral medial frontal, superior frontal, and paracingulate gyri compared to the SCI group. No significant FC differences were found between the MCI and SCI groups (Table 4, Fig. 5). For the right MDm seed, ANCOVA revealed altered FC with the left superior frontal gyrus and right frontal pole across the three groups. Post hoc analyses showed decreased FC with the left superior frontal, medial frontal gyri, and anterior cingulate gyrus in the ADD patients, and bilateral frontal poles in the MCI participants compared to the SCI group (Table 4, Fig. 5). No significant FC differences were found between the ADD and MCI groups.

Table 2
Thalamic nuclei volumetric analysis results.

		Volume-to-eTIV ratio (x10^{-6})					
		SCI	**MCI**	**ADD**	***F (2,74)***	***p***	**η^2**
Right							
	Anterior Group	122.610 ± 4.124	121.463 ± 4.024	112.414 ± 4.938	1.409	0.251[b]	0.037
	Lateral Group	144.740 ± 5.304	138.429 ± 5.175	125.461 ± 6.350	2.645	0.078[b]	0.067
	Ventral Group	2643.007 ± 79.983	2774.311 ± 65.188	2673.967 ± 66.804	0.976	0.382[b]	0.026
	Intralaminar Group	414.196 ± 10.852	424.684 ± 10.589	435.852 ± 12.993	0.784	0.461[b]	0.021
	Medial Group	895.945 ± 15.560	849.173 ± 15.184	784.856 ± 18.630	8.285	**0.001[b]**	0.183
	Posterior Group	1575.322 ± 36.669	1565.617 ± 35.782	1473.850 ± 43.903	1.793	0.174[b]	0.046
Left							
	Anterior Group	110.388 ± 3.725	108.910 ± 3.635	94.230 ± 4.460	4.423	0.015[b]	0.107
	Lateral Group	140.406 ± 5.235	143.598 ± 5.108	119.286 ± 6.268	5.017	0.009[b]	0.119
	Ventral Group	2618.988 ± 59.864	2690.147 ± 58.416	2516.965 ± 71.674	1.775	0.177[b]	0.046
	Intralaminar Group	400.747 ± 11.130	405.554 ± 10.861	412.751 ± 13.325	0.229	0.796[b]	0.006
	Medial Group	931.231 ± 18.918	911.625 ± 18.460	821.063 ± 22.650	7.398	**0.001[b]**	0.167
	Posterior Group	1742.830 ± 40.219	1752.620 ± 39.246	1631.050 ± 48.153	2.205	0.117[b]	0.056

Values shown are in mean ± standard deviation. ANCOVA was performed by controlling the effect of age, education, and gender (Bonferroni-corrected significance threshold of thalamic subgroups [b]***p* < 0.0042** [0.05/12]). SCI: Subjective cognitive impairment; MCI: Mild cognitive impairment; ADD: Alzheimer's disease dementia; R: Right; L: Left.

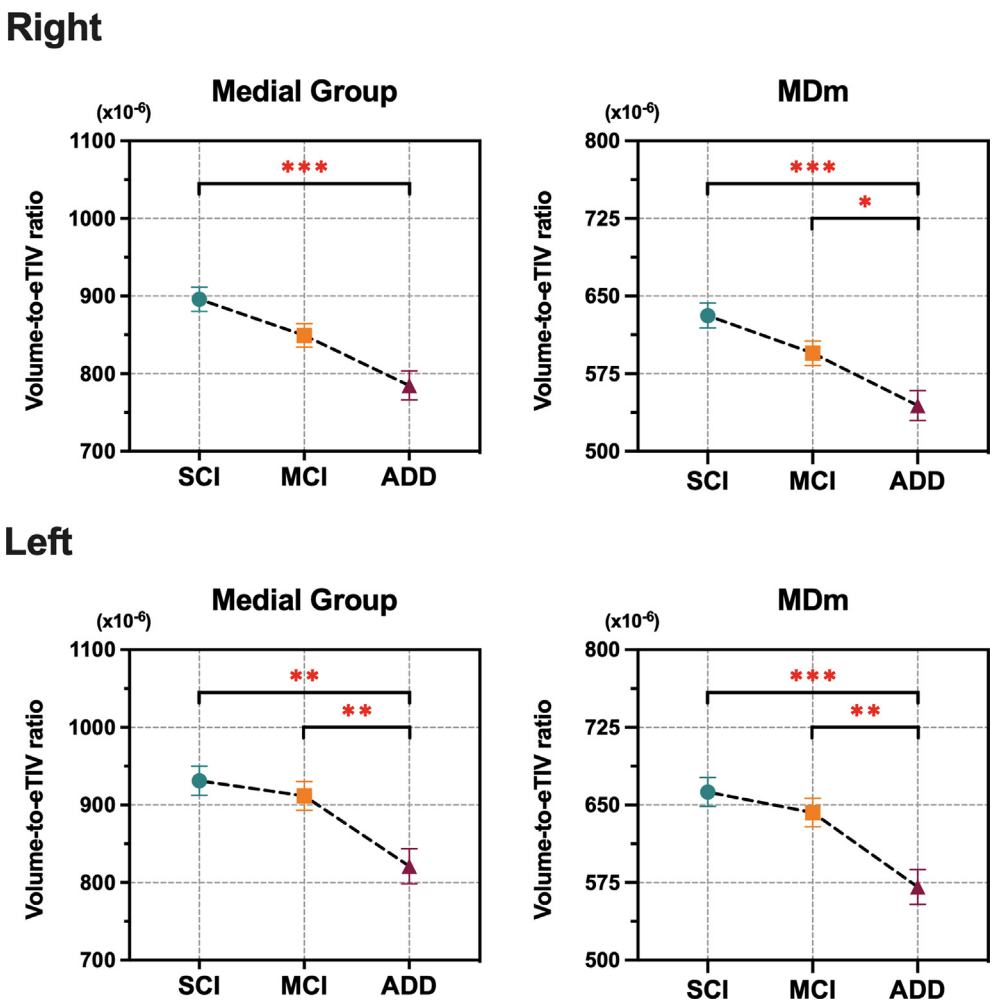


Fig. 3. Post hoc comparisons of anatomical regions with significant differences as a result of ANCOVA between 3 clinical groups. Mean volumes to eTIV ratios have been reported (Bonferroni-corrected significance threshold $^{*}p < 0.05$; $^{**}p < 0.01$; $^{***}p < 0.001$). MDm: Mediodorsal medial magnocellular; SCI: Subjective cognitive impairment; MCI: Mild cognitive impairment; ADD: Alzheimer's disease dementia.

Table 3
Volumetric findings for the thalamic nuclei within the medial group.

	Volume-to-eTIV ratio (x10^{-6})					
	SCI	**MCI**	**ADD**	***F (2,74)***	***p***	**η^2**
Right						
MDl	247.961 ± 4.959	238.030 ± 4.839	234.948 ± 5.937	1.581	0.213	0.041
MDm	631.047 ± 12.029	594.725 ± 11.738	544.330 ± 14.402	10.201	**0.0001***	0.216
MV-Re	10.252 ± 0.458	9.505 ± 0.447	8.869 ± 0.548	1.821	0.169	0.047
Pt	6.685 ± 0.195	6.912 ± 0.190	6.708 ± 0.234	0.399	0.672	0.011
Left						
MDl	251.800 ± 5.787	252.330 ± 5.647	234.666 ± 6.928	2.343	0.103	0.060
MDm	662.631 ± 14.053	642.754 ± 13.713	570.739 ± 16.825	9.073	**0.0002***	0.197
MV-Re	10.087 ± 0.376	9.606 ± 0.367	9.090 ± 0.450	1.385	0.257	0.036
Pt	6.713 ± 0.195	6.935 ± 0.190	6.567 ± 0.233	0.800	0.453	0.021

Values shown are in mean ± standard deviation. ANCOVA was performed by controlling the effect of age, education, and gender (Bonferroni-corrected significance threshold of thalamic subnuclei $^{*}\boldsymbol{p < 0.001}$ [0.05/50]). SCI: Subjective cognitive impairment; MCI: Mild cognitive impairment; ADD: Alzheimer's disease dementia; R: Right; L: Left; MDl: Mediodorsal lateral parvocellular; MDm: Mediodorsal medial magnocellular; MV-Re: Medial ventral-reuniens; Pt: Paratenial.

4. Discussion

In this study, it was aimed to examine the volumetric and functional connectivity changes between SCI, MCI and ADD groups of the specific nuclei of the thalamus, which is a very heterogeneous structure histologically and functionally. As a result of volumetric and functional connectivity analyses, our findings indicated that MD nuclei were affected in AD. MDm, the main paralimbic cortices-related thalamic nucleus was indeed becoming smaller and altering its pattern of connectivity along the disease course. But this shrinkage/misconnection became significant only in the dementia stage compared to both pre-dementia stages (SCI and MCI). The modality-specific cortices-related nuclei indeed showed no differences among the groups. MDm did not differ between SCI

Table 4
The functional connectivity differences between groups.

Seed Regions	Contrast	MNI Coordinate	Cluster Size	Regions	p_{FWE}
L Medial Group	Group differences	04, 38, 38	482	R-Paracingulate gyrus, R-SFG	0.000672
		-20, 24, 56	365	L-SFG	0.003579
		28, 32, 50	286	R-MFG, R-SFG	0.012242
	ADD > MCI	28, -46, -04	1077	R-Lingual gyrus, R-Intracalcarine cortex	0.000008
		16, -82, 40	523	R-Lateral occipital cortex, R-Cuneal cortex	0.001765
		–22, -50, -02	381	L-Lingual gyrus	0.009163
	ADD < SCI	04, 36, 38	1626	R-SFG, R-MFG, R-Paracingulate gyrus, L-Paracingulate gyrus, R-FP	<0.000001
		-20, 24, 56	612	L-SFG, L-MFG	0.000729
L MDm	Group differences	04, 38, 38	453	R-Paracingulate gyrus, R-SFG	0.001027
		-20, 24, 56	356	L-SFG	0.004180
	ADD > MCI	28, -46, -4	1059	R-Lingual gyrus, R-Intracalcarine cortex	0.000009
		16, -82, 40	756	R-Lateral occipital cortex, R-Cuneal cortex, R-OP	0.000144
		-26, -58, -12	356	L-Lingual gyrus	0.011860
	ADD < SCI	04, 38, 38	1466	R-MFG, R-SFG, R-Paracingulate gyrus, L-Paracingulate gyrus	<0.000001
		-20, 24, 56	716	L-SFG, L-MFG	0.000254
R Medial Group	Group differences	-24, 34, 44	354	L-SFG	0.004657
	ADD < SCI	–22, 34, 46	616	L-SFG, L-MFG	0.000809
		32, 32, 50	350	R-MFG	0.015430
		02, 42, 30	347	R-Paracingulate gyrus	0.016006
R MDm	Group differences	–22, 23, 44	358	L-SFG	0.003962
		08, 56, 08	301	R-FP	0.009589
	MCI < SCI	08, 56, 08	363	L-FP, R-FP	0.012550
	ADD < SCI	–22, 34, 46	583	L-SFG, L-MFG	0.001041
		-12, 54, 08	529	Anterior cingulate gyrus	0.001850

SCI: Subjective cognitive impairment; MCI: Mild cognitive impairment; ADD: Alzheimer's disease dementia; MDm: Mediodorsal medial magnocellular; SFG: Superior frontal gyrus; MFG: Middle frontal gyrus; FP: Frontal pole; OP: Occipital pole; R: Right; L: Left; FWE: Family-wise error; MNI: Montreal Neurological Institute. The threshold for ANOVA analysis was set to $p < 0.001$ at the voxel level and $p_{FWE} < 0.0125$ at the cluster level. Bonferroni correction was applied for pairwise comparisons, and the significance threshold was set at $p_{FWE} < 0.017$.

and MCI, despite a trend. ATN, the main limbic-related thalamic nuclei, and MDl/PuM, the main heteromodal thalamic nuclei were not discriminatory among the groups, again despite trends.

In the functional connectivity analyses in which medial group nuclei and MDm were selected as ROIs, both ADD and MCI patients displayed significantly decreased functional connectivity to the frontal areas in comparison to the SCI participants. Whereas, both the medial group and MDm increased their functional connectivity to the visual areas in the ADD group, compared to the MCI group. Our findings suggest that thalamo-cortical connections are affected in AD and this pattern of influence is associated with the course of the disease.

MDm is also part of the parahippocampal-prefrontal memory system, which includes the perirhinal, parahippocampal, and medial prefrontal cortices (Aggleton, 2012). Lesions observed in experimental animals and humans showed the role of the mediodorsal thalamus in recognition memory (Cross et al., 2013). A study by Pardilla-Delgado et al., 2021, demonstrated no significant difference in thalamic volumes between the AD patients with and without mutation in the PSEN1 E280A gene, however, they found a negative correlation between the medial thalamus and, to a lesser extent, posterior thalamus volumes with both cortical amyloid load and entorhinal cortex tau load (Pardilla-Delgado et al., 2021). Our finding indicating the volumes of the medial group nuclei and MDm accounted for a small to medium proportion of the variance in the memory scores of FCRST-TFR, also supports the role of these thalamic nuclei in memory function.

MDm has also been recognized as reciprocally connected with primary olfactory cortices and higher-order olfactory areas in the orbitofrontal cortex (Courtiol and Wilson, 2015; Tham et al., 2009). In this context, volume reduction in MDm may also contribute to olfactory dysfunction which was frequently reported in AD (Quarmley et al., 2017; Velayudhan et al., 2015; Ward et al., 2017).

The reason for the lack of MDm volume differences between the SCI and MCI groups may be due to the use of only clinical diagnostic criteria and the absence of neurobiological biomarkers in this study. Positive CSF biomarker rates in individuals clinically diagnosed with SCI and MCI have been reported to be 7–24% and 50.1%, respectively (Hwang et al., 2019; Parnetti et al., 2019). On the other hand, the CSF biomarker rate is up to 92% in individuals clinically diagnosed with AD (Hwang et al., 2019). The absence of neurobiological biomarkers can be considered an important limitation of our study, as it has the potential to lead to false positive findings by reducing the volumetric contrast between our SCI and MCI groups.

Due to its location and critical connections in the Papez circuit, the anterior thalamus is important for memory functions (Aggleton et al., 2016). The anterior thalamus is also where the neurofibrillary tangles are observed at the earliest stages of NFT spread. Braak and Braak notes their incidental presence in antero-dorsal nucleus (AD) in their stage I and presence in small amounts in stage II (noted as i and + respectively) (Braak and Braak, 1991). A recent study by Low and colleagues revealed that there was no difference in the anterior thalamus volume between the amyloid-positive MCI and healthy control groups, but in the ADD group compared to the MCIs and healthy controls (Low et al., 2019). Although the anterior thalamus could not recover from conservative Bonferroni

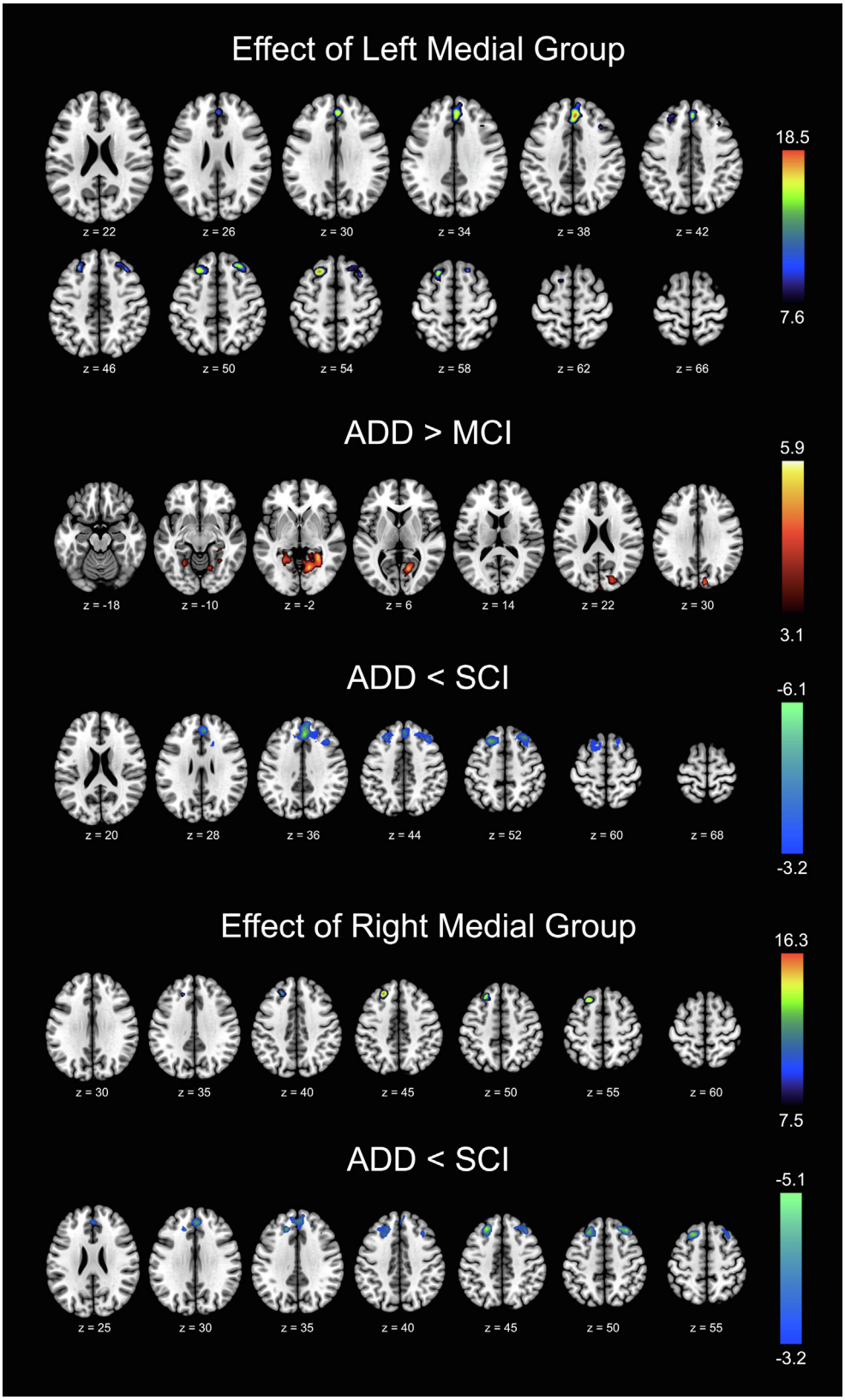


Fig. 4. Functional connectivity differences between 3 clinical groups for medial group nuclei. The threshold for ANOVA analysis was set to $p < 0.001$ at the voxel level and $p_{FWE} < 0.0125$ at the cluster level. Bonferroni correction was applied for pairwise comparisons, and the significance threshold was set at $p_{FWE} < 0.017$. SCI: Subjective cognitive impairment; MCI: Mild cognitive impairment; ADD: Alzheimer's disease dementia.

correction in our study, this may be due to its very small size. In the atlas we used, the "anterior group" nuclei included the antero-dorsal, antero-medial and antero-ventral nuclei, while LD, which was thought to be located within the ATN, was included in the "lateral group" nuclei. The fact that we did not find any discriminatory changes among the groups in pulvinar volumes may be interpreted

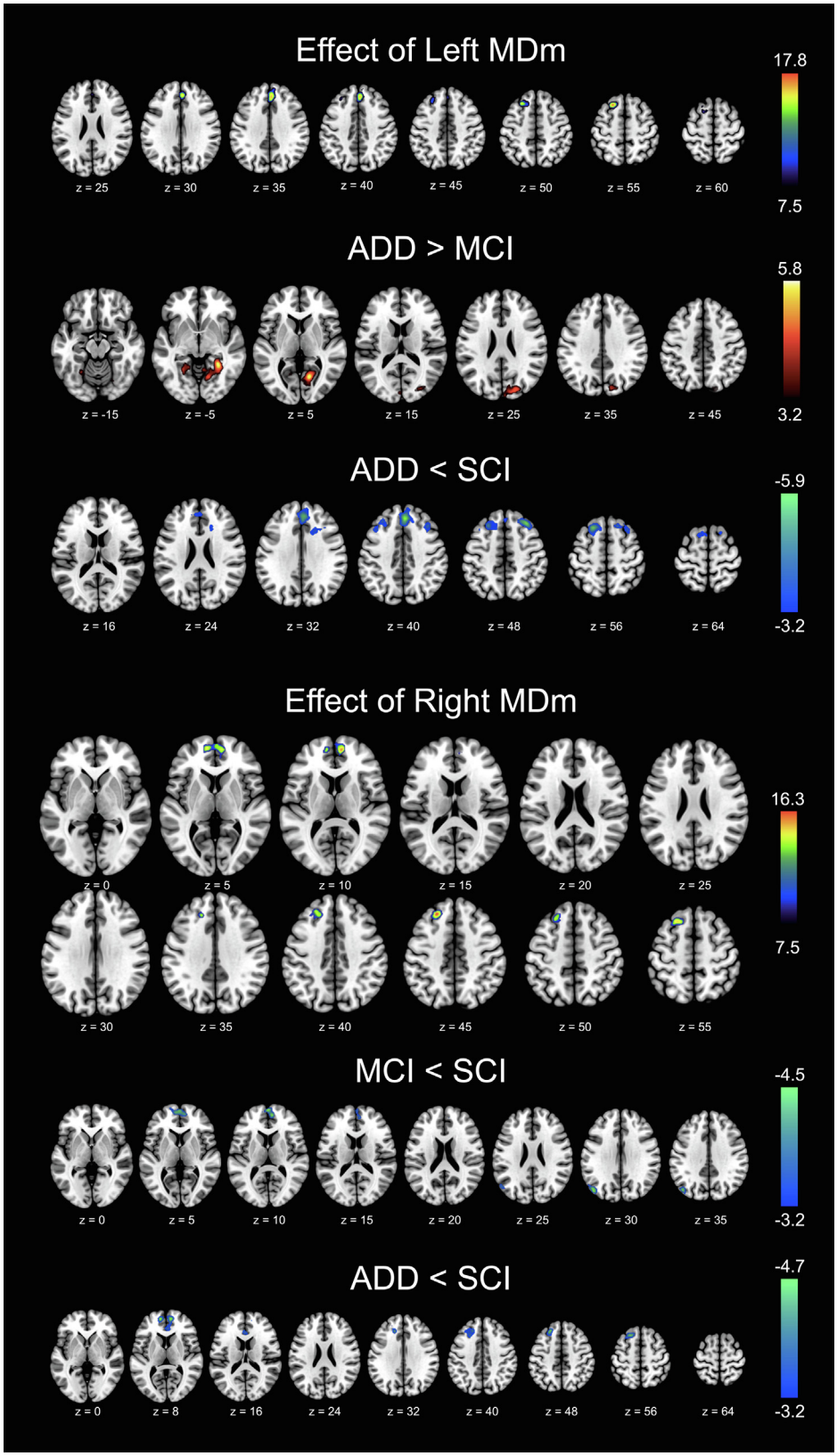


Fig. 5. Functional connectivity differences between 3 clinical groups for mediodorsal medial magnocellular nucleus. The threshold for ANOVA analysis was set to $p < 0.001$ at the voxel level and $p_{FWE} < 0.0125$ at the cluster level. Bonferroni correction was applied for pairwise comparisons, and the significance threshold was set at $p_{FWE} < 0.017$. SCI: Subjective cognitive impairment; MCI: Mild cognitive impairment; ADD: Alzheimer's disease dementia; MDm: Mediodorsal medial.

likewise. The heteromodal nucleus PuM was hidden within the posterior group nuclei along with several first-order (MGN and LGN) and second-order (PuL and PuI) nuclei.

Since the thalamus has highly diverse cortical connections along with its highly heterogeneous substructures, it is not surprising to show functional connectivity changes to widespread cortical structures. In our study, when we examined the functional connectivity changes of the specific subnuclei of the thalamus where the volumetric changes observed in the late stage of the disease, we found that the medial group and its MDm nuclei of both the left and right thalami decreased their functional connectivity to the superior and medial frontal areas in ADD patients compared to the SCI participants, whereas the right MDm nucleus with its decreased functional connectivity with the frontal poles was the only thalamic region that differed the MCI subjects from the SCIs. In addition to the decreasing FC throughout the disease (mostly for SCI vs ADD), the opposite pattern was obtained only for the left medial group and its MDm nuclei seed, where these thalamic areas increased their FC with occipital areas in the ADD patients, compared to the MCIs. This increased FC may indicate a misconnection or a compensatory effort that occurs during the dementia stage of the disease. A similar finding has been previously reported. Cai et al showed that with connectivity decreases in various frontal and temporal areas along the cognitive impairment continuum, there was also thalamo-visual FC (in fusiform gyrus and precuneus) increases in early MCI, and late MCI compared to healthy controls and comparison of two patient groups also revealed an increased connectivity in the late MCI group, which were interpreted as compensatory activity (Cai et al., 2015).

5. Conclusion

In conclusion, the main findings of the study are the decreased connectivity of medial group nuclei and MDm with frontal areas, which may explain the episodic memory deficits seen in the disease. On the other hand, the most critical finding is the reduced functional connectivity between the MDm nucleus and the frontal pole between SCI and MCI, which also provides a clue for an early imaging marker of the disease. FC alterations of the medial group and MDm nuclei of the thalamus with various cortical structures indicate that thalamo-frontal and thalamo-occipital connectivities are conversely affected in the course of AD. These findings demonstrate the importance of focusing on specific sub-nuclei to better understand the course of the disease and suggest the thalamic segmentation algorithm as a useful and sensitive tool to investigate structural and functional changes throughout the disease.

Ethical approval

The study was approved by the Clinical Research Ethics Committee of Istanbul University, Istanbul Faculty of Medicine (Protocol No: 2022/1494). This study was performed in accordance with the ethical principles of the latest version of the Declaration of Helsinki.

Informed consent

Written informed consent was provided by all participants.

Funding

This work was supported by Istanbul University Research Projects Unit (Grant #: 2019K12-149071); Istanbul University Research University Support Program (Grant #: TSA-2022-39128).

Conflict of interest

The authors declare no competing interests.

CRediT authorship contribution statement

Emre Hari: Conceptualization, Methodology, Formal analysis, Investigation, Writing – original draft, Visualization, Writing – review & editing. **Cigdem Ulasoglu-Yildiz:** Conceptualization, Methodology, Formal analysis, Investigation, Writing – original draft, Visualization, Writing – review & editing. **Elif Kurt:** Methodology, Formal analysis, Investigation, Writing – original draft, Visualization, Writing – review & editing. **Ali Bayram:** Methodology, Investigation, Formal analysis, Writing – review & editing. **Hakan Gurvit:** Conceptualization, Formal analysis, Methodology, Resources, Writing – review & editing, Supervision. **Tamer Demiralp:** Conceptualization, Methodology, Resources, Writing – review & editing, Supervision.

Acknowledgements

We thank Burak Acar, Elif Yıldırım and Ezgi Soncu Büyükişcan for their contribution.

Appendix A. Supplementary material

Supplementary material to this article can be found online at https://doi.org/10.1016/j.clinph.2024.06.018.

References

Aggleton JP. Multiple anatomical systems embedded within the primate medial temporal lobe: implications for hippocampal function. Neurosci Biobehav Rev 2012;36:1579–96. https://doi.org/10.1016/j.neubiorev.2011.09.005.

Aggleton JP, Pralus A, Nelson AJD, Hornberger M. Thalamic pathology and memory loss in early Alzheimer's disease: moving the focus from the medial temporal lobe to Papez circuit. Brain 2016;139:1877–90. https://doi.org/10.1093/brain/aww083.

Alves PN, Foulon C, Karolis V, Bzdok D, Margulies DS, Volle E, et al. An improved neuroanatomical model of the default-mode network reconciles previous neuroimaging and neuropathological findings. Commun Biol 2019;2:370. https://doi.org/10.1038/s42003-019-0611-3.

Behzadi Y, Restom K, Liau J, Liu TT. A component based noise correction method (CompCor) for BOLD and perfusion based fMRI. Neuroimage 2007;37:90–101. https://doi.org/10.1016/j.neuroimage.2007.04.042.

Bernstein AS, Rapcsak SZ, Hornberger M, Saranathan M, Initiative ADN. Structural changes in thalamic nuclei across prodromal and clinical Alzheimer's disease. J Alzheimer's Dis 2021;82:361–71. https://doi.org/10.3233/JAD-201583.

Bobinski M, De Leon MJ, Wegiel J, Desanti S, Convit A, Saint Louis LA, et al. The histological validation of post mortem magnetic resonance imaging-determined hippocampal volume in Alzheimer's disease. Neuroscience 1999;95:721–5. https://doi.org/10.1016/S0306-4522(99)00476-5.

Braak H, Braak E. Neuropathological stageing of Alzheimer-related changes. Acta Neuropathol 1991;82:239–59. https://doi.org/10.1007/BF00308809.

Braak H, Thal DR, Ghebremedhin E, Del Tredici K. Stages of the pathologic process in Alzheimer disease: age categories from 1 to 100 years. J Neuropathol Exp Neurol 2011;70:960–9. https://doi.org/10.1097/NEN.0b013e318232a379.

Buckner RL, Krienen FM, Castellanos A, Diaz JC, Yeo BTT. The organization of the human cerebellum estimated by intrinsic functional connectivity. J Neurophysiol 2011;106:2322–45. https://doi.org/10.1152/jn.00339.2011.

Buschke H. Cued recall in amnesia. J Clin Neuropsychol 1984;6:433–40. https://doi.org/10.1080/01688638408401233.

Cai S, Huang L, Zou J, Jing L, Zhai B, Ji G, et al. Changes in thalamic connectivity in the early and late stages of amnestic mild cognitive impairment: a resting-state functional magnetic resonance study from ADNI. PLoS One 2015;10:e0115573.

Choi EY, Yeo BTT, Buckner RL. The organization of the human striatum estimated by intrinsic functional connectivity. J Neurophysiol 2012;108:2242–63. https://doi.org/10.1152/jn.00270.2012.

Cipolotti L, Husain M, Crinion J, Bird CM, Khan SS, Losseff N, et al. The role of the thalamus in amnesia: A tractography, high-resolution MRI and neuropsychological study. Neuropsychologia 2008;46:2745–58. https://doi.org/10.1016/j.neuropsychologia.2008.05.009.

Courtiol E, Wilson DA. The olfactory thalamus: unanswered questions about the role of the mediodorsal thalamic nucleus in olfaction. Front Neural Circuits 2015;9:49. https://doi.org/10.3389/fncir.2015.00049.

Cross L, Brown MW, Aggleton JP, Warburton EC. The medial dorsal thalamic nucleus and the medial prefrontal cortex of the rat function together to support associative recognition and recency but not item recognition. Learn Mem 2013;20:41–50. https://doi.org/10.1101/lm.028266.112.

Danet L, Barbeau EJ, Eustache P, Planton M, Raposo N, Sibon I, et al. Thalamic amnesia after infarct. Neurology 2015;85:2107–15. https://doi.org/10.1212/WNL.0000000000002226.

Ertan T, Eker E, ar V. Geriatrik depresyon ölçeğinin Türk yaşlı nüfusunda geçerlilik ve güvenilirliği. Nöropsikiyatri Arşivi 1997;34:62–71.

Fischl B, Salat DH, Busa E, Albert M, Dieterich M, Haselgrove C, et al. Whole brain segmentation: automated labeling of neuroanatomical structures in the human brain. Neuron 2002;33:341–55. https://doi.org/10.1016/s0896-6273(02)00569-x.

Folstein MF, Folstein SE, McHugh PR. "Mini-mental state". A practical method for grading the cognitive state of patients for the clinician. J Psychiatr Res 1975;12:189–98. https://doi.org/10.1016/0022-3956(75)90026-6.

Friston KJ, Ashburner J, Frith CD, Poline J, Heather JD, Frackowiak RSJ. Spatial registration and normalization of images. Hum Brain Mapp 1995;3:165–89. https://doi.org/10.1002/hbm.460030303.

Grober E, Sanders AE, Hall C, Lipton RB. Free and cued selective reminding identifies very mild dementia in primary care. Alzheimer Dis Assoc Disord 2010;24:284–90. https://doi.org/10.1097/WAD.0b013e3181cfc78b.

Hwang J, Jeong JH, Yoon SJ, Park KW, Kim E-J, Yoon B, et al. Clinical and biomarker characteristics according to clinical spectrum of Alzheimer's disease (AD) in the validation cohort of Korean brain aging study for the early diagnosis and prediction of AD. J Clin Med 2019;8:341. https://doi.org/10.3390/jcm8030341.

Hwang K, Bertolero MA, Liu WB, D'Esposito M. The human thalamus is an integrative hub for functional brain networks. J Neurosci 2017;37:5594. https://doi.org/10.1523/JNEUROSCI.0067-17.2017.

Iglesias JE, Insausti R, Lerma-Usabiaga G, Bocchetta M, Van Leemput K, Greve DN, et al. A probabilistic atlas of the human thalamic nuclei combining ex vivo MRI and histology. Neuroimage 2018;183:314–26. https://doi.org/10.1016/j.neuroimage.2018.08.012.

Ivnik RJ, Smith GE, Lucas JA, Tangalos EG, Kokmen E, Petersen RC. Free and cued selective reminding test: MOANS norms. J Clin Exp Neuropsychol 1997;19:676–91. https://doi.org/10.1080/01688639708403753.

Jack CRJ, Knopman DS, Jagust WJ, Shaw LM, Aisen PS, Weiner MW, et al. Hypothetical model of dynamic biomarkers of the Alzheimer's pathological cascade. Lancet Neurol 2010;9:119–28. https://doi.org/10.1016/S1474-4422(09)70299-6.

Jagirdar R, Chin J. Corticothalamic network dysfunction and Alzheimer's disease. Brain Res 2019;1702:38–45. https://doi.org/10.1016/j.brainres.2017.09.014.

Jessen F, Amariglio RE, Van Boxtel M, Breteler M, Ceccaldi M, Chételat G, et al. A conceptual framework for research on subjective cognitive decline in preclinical Alzheimer's disease. Alzheimers Dement 2014;10:844–52. https://doi.org/10.1016/j.jalz.2014.01.001.

Low A, Mak E, Malpetti M, Chouliaras L, Nicastro N, Su L, et al. Asymmetrical atrophy of thalamic subnuclei in Alzheimer's disease and amyloid-positive mild cognitive impairment is associated with key clinical features. Alzheimer's & Dementia: Diagnosis, Assessment & Disease Monitoring 2019;11:690–9. https://doi.org/10.1016/j.dadm.2019.08.001.

McKhann GM, Knopman DS, Chertkow H, Hyman BT, Jack CRJ, Kawas CH, et al. The diagnosis of dementia due to Alzheimer's disease: recommendations from the National Institute on aging-Alzheimer's association workgroups on diagnostic guidelines for Alzheimer's disease. Alzheimers Dement 2011;7:263–9. https://doi.org/10.1016/j.jalz.2011.03.005.

Mesulam M-M. Large-scale neurocognitive networks and distributed processing for attention, language, and memory. Ann Neurol 1990;28:597–613. https://doi.org/10.1002/ana.410280502.

Mitchell A, Chakraborty S. What does the mediodorsal thalamus do? Front Syst Neurosci 2013;7. https://doi.org/10.3389/fnsys.2013.00037.

Mitchell AS. The mediodorsal thalamus as a higher order thalamic relay nucleus important for learning and decision-making. Neurosci Biobehav Rev 2015;54:76–88. https://doi.org/10.1016/j.neubiorev.2015.03.001.

Morris JC. The clinical dementia rating (cdr): Current version and. Young 1991;41:1588–92. https://doi.org/10.1212/WNL.43.11.2412-a.

Nieto-Castanon A. Handbook of functional connectivity magnetic resonance imaging methods in CONN. Hilbert Press; 2020.

Pardilla-Delgado E, Torrico-Teave H, Sanchez JS, Ramirez-Gomez LA, Baena A, Bocanegra Y, et al. Associations between subregional thalamic volume and brain pathology in autosomal dominant Alzheimer's disease. Brain Commun 2021;3:fcab101.. https://doi.org/10.1093/braincomms/fcab101.

Parnetti L, Chipi E, Salvadori N, D'Andrea K, Eusebi P. Prevalence and risk of progression of preclinical Alzheimer's disease stages: a systematic review and meta-analysis. Alzheimers Res Ther 2019;11:7. https://doi.org/10.1186/s13195-018-0459-7.

Penny WD, Friston KJ, Ashburner JT, Kiebel SJ, Nichols TE. Statistical parametric mapping: the analysis of functional brain images. Elsevier; 2011.

Pergola G, Danet L, Pitel A-L, Carlesimo GA, Segobin S, Pariente J, et al. The regulatory role of the human mediodorsal thalamus. Trends Cogn Sci 2018;22:1011–25. https://doi.org/10.1016/j.tics.2018.08.006.

Petersen RC. Mild cognitive impairment as a diagnostic entity. J Intern Med 2004;256:183–94. https://doi.org/10.1111/j.1365-2796.2004.01388.x.

Quarmley M, Moberg PJ, Mechanic-Hamilton D, Kabadi S, Arnold SE, Wolk DA, et al. Odor identification screening improves diagnostic classification in incipient Alzheimer's disease. J Alzheimer's Dis 2017;55:1497–507. https://doi.org/10.3233/JAD-160842.

Roh JH, Qiu A, Seo SW, Soon HW, Kim JH, Kim GH, et al. Volume reduction in subcortical regions according to severity of Alzheimer's disease. J Neurol 2011;258:1013–20. https://doi.org/10.1007/s00415-010-5872-1.

Ryan NS, Keihaninejad S, Shakespeare TJ, Lehmann M, Crutch SJ, Malone IB, et al. Magnetic resonance imaging evidence for presymptomatic change in thalamus and caudate in familial Alzheimer's disease. Brain 2013;136:1399–414. https://doi.org/10.1093/brain/awt065.

Scheltens P, Leys D, Barkhof F, Huglo D, Weinstein HC, Vermersch P, et al. Atrophy of medial temporal lobes on MRI in" probable" Alzheimer's disease and normal ageing: diagnostic value and neuropsychological correlates. J Neurol Neurosurg Psychiatry 1992;55:967–72. https://doi.org/10.1136/jnnp.55.10.967.

Schmahmann JD. Vascular syndromes of the thalamus. Stroke 2003;34:2264–78. https://doi.org/10.1161/01.STR.0000087786.38997.9E.

Shi F, Liu B, Zhou Y, Yu C, Jiang T. Hippocampal volume and asymmetry in mild cognitive impairment and Alzheimer's disease: meta-analyses of MRI studies. Hippocampus 2009;19:1055–64. https://doi.org/10.1002/hipo.20573.

Spreng RN, Stevens WD, Chamberlain JP, Gilmore AW, Schacter DL. Default network activity, coupled with the frontoparietal control network, supports goal-directed cognition. Neuroimage 2010;53:303–17. https://doi.org/10.1016/j.neuroimage.2010.06.016.

Tham WWP, Stevenson RJ, Miller LA. The functional role of the medio dorsal thalamic nucleus in olfaction. Brain Res Rev 2009;62:109–26. https://doi.org/10.1016/j.brainresrev.2009.09.007.

Velayudhan L, Gasper A, Pritchard M, Baillon S, Messer C, Proitsi P. Pattern of Smell Identification Impairment in Alzheimer's Disease. J Alzheimer's Dis 2015;46:381–7. https://doi.org/10.3233/JAD-142838.

Ward AM, Calamia M, Thiemann E, Dunlap J, Tranel D. Association between olfaction and higher cortical functions in Alzheimer's disease, mild cognitive impairment, and healthy older adults. J Clin Exp Neuropsychol 2017;39:646–58. https://doi.org/10.1080/13803395.2016.1253667.

Whitfield-Gabrieli S, Nieto-Castanon A. Conn: a functional connectivity toolbox for correlated and anticorrelated brain networks. Brain Connect 2012;2:125–41. https://doi.org/10.1089/brain.2012.0073.

Yeo BTT, Krienen FM, Sepulcre J, Sabuncu MR, Lashkari D, Hollinshead M, et al. The organization of the human cerebral cortex estimated by intrinsic functional connectivity. J Neurophysiol 2011. https://doi.org/10.1152/jn.00338.2011.

Yesavage JA, Brink TL, Rose TL, Lum O, Huang V, Adey M, et al. Development and validation of a geriatric depression screening scale: a preliminary report. J Psychiatr Res 1982;17:37–49. https://doi.org/10.1016/0022-3956(82)90033-4.

Zhou J, Seeley WW. Network dysfunction in Alzheimer's disease and frontotemporal dementia: implications for psychiatry. Biol Psychiatry 2014;75:565–73. https://doi.org/10.1016/j.biopsych.2014.01.020.

Zidan M, Boban J, Bjelan M, Todorović A, Vujanić TS, Semnic M, et al. Thalamic volume loss as an early sign of amnestic mild cognitive impairment. J Clin Neurosci 2019;68:168–73. https://doi.org/10.1016/j.jocn.2019.07.004.